CPW-Fed Dual Band Dual Polarized Antenna for Wearable Applications

Anshul Shrivastava*[1], Ajay Yadav*[2], and Rajesh Kumar[1]

[1]Department of Electronics and Communication Engineering, North Eastern Regional Institute of Science & Technology, Itanagar, 791109, AP, India
[2]Department of Microwave Design, MAASTEK Technologies, Jaipur, Rajasthan, India

KEYWORDS
Circular slot,
Dual band antenna,
Axial ratio,
Wearable applications,
WBAN

Abstract This manuscript analyses a Coplanar Waveguide (CPW) fed ground-slotted antenna for dual-frequency operations. The proposed design comprises a ground circular slot and a modified angular ring with two added strips to obtain dual operating bands and polarization characteristics. The proposed structure is printed on an FR-4 epoxy substrate with a thickness (h) of 1.6 mm and ε_r = 4.4. The overall antenna size is 32×32 mm^2. The measured reflection coefficient, axial ratio, gain, and radiation pattern are in good agreement with simulated results. The lower band operated at 2450 MHz frequency with impedance bandwidths of 275 MHz (from 2350 MHz–2625 MHz) and linearly polarized (LP), and the upper band operated at 5200 MHz with 500 MHz (from 4950 MHz–5450 MHz) operation band coverage and circularly polarized (CP). The upper band is circularly polarized with a 3 dB axial bandwidth from 4850 to 5400 MHz. The designed structure is suitable for on and off-body applications in lower and upper bands, respectively. The proposed antenna characteristics have also been examined on the human arm, and analysis of the Specific Absorption Rate (SAR) to ensure human tissue safety.

1. Introduction

ADVANCED wireless wearable systems require smaller RF components and devices with high data rate handling ability to transmit physiological signals. The antenna is one of the fundamental mechanisms for such devices for wireless communication with compact size and multiband operation. Besides this, specific radiation patterns are desirable for a particular domain of operation, like an omnidirectional pattern for on-body communication and a broadside pattern for off-body communication. In off-body mode, circular polarization (CP) is highly suitable to reduce the losses caused by linear polarization (LP) mismatching [1].

Human tissues may influence WBAN antenna performance [2], which may cause frequency shifts and impedance mismatch due to its large permittivity. The high dielectric constant of the human body's skin might degrade radiation patterns and decrease the gain and efficiency of on-body antennas. Therefore, designing on-body antennas with robust, compact size and low Specific Absorption Rate (SAR) has been challenging. Various wearable antennas have been reported for WBAN applications in the last twenty years. For instance, single-band substrate integrated waveguide (SIW) antennas [3-4].

Corresponding author:
E-mails: anshulnri@gmail.com, ajayrfmicrowave@gmail.com,
Contact No. : 9166877787

Address: Anshul Shrivastava, 708 Aditya Residency, Hurawali Road, Gwalior-474011

Dual-mode antennas with different radiation characteristics are highly needed to enable wearable devices to communicate with both on-body and external nodes. For instance, some button antennas [5-6] which have structure complexity. Using a circular patch, authors realized omnidirectional radiation in TM01 mode, TM02 mode, generation, and zeroth-order mode [7]. However, the gain of the antenna in these modes is low. Besides these, dual-band antennas are preferred for wearable applications. Using shorting pins, angular ring configuration, and multi-layered patches, investigators designed dual-band dual-mode antennas for on and off-body communication [8-11]. A pattern reconfigurable antenna has been presented in [12], which switches the pattern from omnidirectional to a broadside radiation pattern, respectively. Recently, in studies [13-14], authors used capacitive coupling to generate high-order modes and for ON/ OFF body antenna design. However, these reports are mainly excited by probe-fed technique, which is unsuitable for wearable applications. Furthermore, some researchers designed dual-band antennas using coplanar waveguide-fed [15-16] and microstrip-fed lines [17-21]. But on- and off-body domain antennas must work simultaneously in two modes. So, to increase system communication link reliability, the antenna needs to be operated with dual polarization characteristics [22]. Some dual-mode dual-polarized antennas [23-25] and dual-band circular polarized antennas [26-27] have been designed for wearable applications. However, above mentioned structures have large footprints and complex designs.

In this study, a dual-band dual-polarized antenna has been proposed for ON and OFF-body communication. The antenna design utilized a modified angular ring patch with inverted T-shaped strips and a circular slot in the ground plane to produce the dual-band and dual-polarized characteristics at 2.45 GHz and 5.2 GHz frequencies. The inverted T-shaped strip is mainly responsible for generating CP in the upper-frequency band. Section II discussed antenna design and working mechanism. Section III provides the details of fabrication and measurements. Section IV represents the on-body analysis with SAR calculation**.**

The proposed antenna has the following features

1. The proposed antenna has a low profile and simple structure compared to [18-20][22-25].
2. The antenna has dual-band operation with a compact size of 32 x 32 mm^2. The proposed antenna shows reasonable reflection coefficients (S_{11}) in two bands from 2350 MHz–2625 MHz and from 4950 MHz–5450 MHz, with a minimum S_{11} of -18 dB at 2450 MHz and -22 dB at 5200 MHz.
3. The proposed antenna has dual polarization characteristics, i.e., linearly polarized in the first band and circularly polarized in the second band, which enables the antenna to operate in dual modes in ON-body and OFF-body modes. So, a single antenna can be utilized for dual operations in the WBAN system.
4. The proposed antenna has slotted circular ring and circular etched ground structure, which makes it very convenient to control the antenna effective inductance and capacitance in radiation. The

proposed structure has benefits of smooth capacitance and inductance to resonate the antenna at desired frequencies, whereas other discontinuities may provide sharp variation in capacitance/inductance values. The proposed shape of antenna may useful for the future research to achieve the desired resonance frequency and circular polarization.

5. The proposed antenna may satisfactorily work near human proximity and utilized for healthcare applications, IoT applications, and tracking in the future.

2. Dual Band Dual Polarized Antenna Design and Analysis

The geometry of the CPW-fed circular slotted dual band antenna is depicted in Fig. 1. The proposed antenna is printed on a glass epoxy FR-4 square-shaped dielectric substrate. The thickness of the substrate is 1.6 mm, relative permittivity is 4.4, and loss tangent tanδ is 0.02. The overall footprint of the proposed dual-band antenna is 32 x 32 mm^2 with a circular-shaped slot in the ground plane of radius R_1 = 13.9 mm. A modified angular shape with two added strip patches is excited by the CPW-fed line. The width W_f = 2.4 mm of the fed line is used to match the 50 ohm impedance of the input port. The modified angular ring with two strips is the main feature to achieve dual-band operation and circular polarization in the upper band, which drives the structure in dual modes for the WBAN system. To provide the wide Axial Ratio Band Width (ARBW), a modified annular ring-shaped monopole radiating part with inverted T-shaped strips is utilized to generate CP mode at a higher frequency by splitting the fundamental mode into two near-degenerative modes with equal amplitude and 90^0 phase difference for off-body communication. The commercially available CST microwave studio software performs all numerical analyses of the designed dual-band antenna. The optimized dimensions of the proposed antenna are tabulated in Table 1.

2.1 Step-by-Step Development of Dual Band Dual Polarized Antenna Design:

In order to reach the desired antenna feature, i.e., dual-band and dual-polarized characteristics, the proposed design has been evaluated in four steps, as displayed in Fig. 2. Fig 3 represents the simulated results of the antenna in terms of the reflection coefficient (S_{11}), and Fig. 4 depicts the axial ratio (AR) of namely Antenna 1; Antenna 2, Antenna 3 and Antenna 4 (Final Design). It is observed from Fig.2 (a) that Antenna 1 has simply a circular slot in the ground plane and circular patch, which resonated at nearly 3.5 GHz. In the next step, the circular patch is converted into a modified angular ring-shaped radiator (as Antenna 2 depicted in Fig.2 (b). The Antenna 2 helps to achieve dual-band characteristics along with linear polarization but not in desired bands. Furthermore, to obtain a dual band at 2.45 GHz and another at 5.2 GHz, two strips are added with an angular ring, as shown in Fig.2 (c), but these strips cannot generate CP characteristics. In the final design (Antenna 4), strips are modified as an inverted T shape, enhancing impedance matching and generating the CP characteristics in the higher frequency band. The final antenna resonated in two bands at 2.45 GHz with band coverage from 2.35 GHz to 2.625 GHz and at 5.2 GHz from 4.95 to 5.45 GHz.

2.2 Working Mechanism of the Proposed Design

In this section, the working mechanism of the proposed antenna is described with the help of the current distribution. Fig. 5 depicts the current distribution at 2.45 GHz and 5.2 GHz, as shown in Fig.5 (a) major current radiated along the circular slot in the ground, but in Fig.5 (b) maximum current distributed near the angular ring and inverted T strips. Besides this, Fig.6 (a to d) shows the distribution of current at *t = T/4, t =T/2, t = 3T4, and t = T*. It is seen from Fig.6 that the current rotates in a clockwise direction over a given time which produces right-handed circle polarization (RHCP).

2.3 Parametric Study

In the proposed antenna, the dual-band resonate frequency and circular polarization are affected by the modified annular ring patch and inverted T-shaped strips. However, to verify this, the effects on various parameters like impedance bandwidth and ARs are carried out by changing the angular ring width and total angular arc length. The width sets the size of the inverted T strip, so by varying R_3, it changes the L_2, which plays a critical role in setting dual band characteristics at 2.45 GHz and 5.2 GHz, as seen in Fig. 7(a). The optimized value is 10.2 mm, which fixes the L_2 at 5.85 mm, which sets the upper band at 5.2 GHz and improves impedance in both bands. As depicted in Fig. 7(b), the axial ratio is also improved in the upper band at this dimension. At the time of the parametric study, only one parameter varies at a time, with a value of the others as fixed.

The total arc length of L_{arc} mainly affects the resonating frequency and lower band impedance matching shown in Fig.8 (a). It can easily be observed from Fig.8 (b) that total arc length does not much affect AR at the upper-frequency band, with only slight variations noticed at 5.2 GHz frequency.

2.4 Equivalent Circuit of the Proposed Antenna

The proposed antenna is also modeled by a simple equivalent electrical circuit model, as depicted in Fig. 9(a). [28]. The CPW fed line is modeled by discrete elements R_1, L_1, and C_1. The capacitor C_c represents the slot coupling. Two parallel RLC circuits are connected in series to obtain the dual-band operation, and a parallel combination of L and C is modeled as the slot in a circular monopole radiator. A comparison of the reflection coefficient obtained from the full-wave EM simulator and the equivalent circuit is shown in Fig. 9(b) and observed a close agreement between both.

3. Fabrication and Measurement

The designed dual-band dual-polarized antenna has been measured by Agilent Vector Network Analyzer (VNA) as set up displayed in Fig.10. The antenna performance in terms of reflection coefficient, axial ratio, radiation pattern, and gain is measured in free space and on the human body also to validate, the suitability of the fabricated prototype close human proximity.

3.1 Reflection Coefficient and Axial Ratio

The simulated and measured reflection coefficient represented in Fig.11 observed a good agreement between both results except for slight bandwidth variation due to fabrication and measurement errors. The simulated and measured impedance bandwidth in lower operating bands below -10 dB is 15.67% and 11.22 %, centered at 2.45 GHz, respectively. Similarly, simulated and measured impedance bandwidth for the upper band is 6.46 % and 9.6 %, centered at 5.2 GHz, respectively, as depicted in Fig 12. Besides this, the AR simulated and measured bandwidth is 10.5% (4.85 to 5.4 GHz) and 10% (4.98 to 5.5 GHz).

3.2 Radiation Pattern and Gain

Fig. 13 and Fig. 14, exhibited the far field radiation patterns at phi 0^0 and phi 90^0 for the lower and upper bands, respectively. It is noticed that the antenna exhibits an omnidirectional radiation pattern in the lower band in both planes and RHCP and LHCP for the upper band, which proves the utility of the designed antenna for the WBAN system for simultaneous on and OFF-body communication.

4. ON Body Performance And SAR Analysis

The design was placed on a human phantom arm to validate the specific absorption rate characteristics of the antenna, and the performance parameters, such as S_{11} and AR, were analyzed. All investigations have been carried out by placing the antenna on a human phantom in the built model" HUGO" in the CST simulator, as presented in Fig.15.

Fig. 16 shows the antenna performance with or without the phantom and with different separation distances. When the antenna is in free space, S_{11} of the antenna is less than −10 dB for frequencies from 2350 MHz–2625 MHz and from 4950 MHz–5450 MHz. But when the antenna is placed on the human arm at 1 gap, the antenna S_{11} is significantly affected in both bands. The resonating frequencies are shifted slightly with changed reflection coefficients. The variation in the reflection coefficient is due to the high dielectric constant of the human skin tissue. As the gap between the antenna and body increases, i.e., 5 mm, the antenna reflection coefficients have not significantly detuned, as depicted in Fig.16. Similarly, analysis has also been carried out with cotton cloth on the human arm to validate the performance of the proposed antenna in real implementation when the antenna placed on the human body. For this analysis, a cotton cloth with a dielectric constant of 1.7 and a loss tangent of 0.07 is used in the simulation setup. It is noticed that there is no significant change in resonating frequencies, as shown in Fig.17 (a). Fig. 17(b), shows the variation in axial coefficient on the human arm with and without cotton cloth. The 3 dB bandwidth is slightly reduced with cotton cloth due to its own dielectric constant. But the dielectric constant of cloth is low, that's why it produces less effect on the antenna performance.

The fabricated prototype is tested on a female body arm for the reflection coefficient. To install the antenna on the body arm, the loose-fitting cloth is used to maintain the gap between the antenna and the human body. Paper tape is utilized to install the antenna on the human body because paper tape has a thin layer and less affects the antenna performance. Notable, to measure the axial ratio with the human arm, an arm mimicking the phantom is used. The prepared gel, which the recipe is given in [29], is placed in a plastic container. At the measurement, the antenna is kept in a container and set inside an anechoic chamber. The electrical properties of the mimic are taken from [30], as mentioned in Table 2.

According to Fig. 18 and Fig.19, the measured results on the human arm match well with free space results and show good immunity to the influence of the human body. There is a slight variation in impedance bandwidths due to impedance detuning in the presence of human dielectric tissues and dielectric variation in the simulation model and natural body skin.

As the designed WBAN antenna radiates electromagnetic radiation toward the human body, to ensure human safety from these radiations, SAR analysis needs to be examined on the imported HUGO voxel model. The SAR shows the exposure level of wireless devices, which indicates the hazards generated by EM waves. The absorbed electric field by the human body gives the value of SAR, which is proportional to the squared electric field strength value induced in the body.

SAR values can be evaluated either over the whole body (average SAR) or for a small sample, i.e., 1 g or 10 g of tissues[31]. The higher the SAR value, the more EM power is absorbed by the human body tissues and, thus, the more heat is produced in the human body. According to IEEE C95.1-1999 guidelines standards, SAR should be less than 1.6 W/Kg for 1g tissues and 2 W/Kg for 10 g tissues. The SAR is expressed as equation [30]

$$SAR = \frac{P_i}{\rho_i} = \frac{\sigma_i |E|^2}{\rho_i} \quad \text{...(1)}$$

Where, P_i = Power loss density ($Watt/m^3$)

ρ_i = Density of mass (Kg/m^3)

σ_i = Tissue conductivity (S/m) and

E= Induced electric power($\frac{Volts}{m}$)

Two approaches are used to perform SAR calculations: (i) point SAR, and (ii) averaging SAR (mass or volume).

Point SAR is the value without mass averaging and is defined as the maximum SAR of all the grid cells, and point SAR for each grid cell is calculated by absorbed power in each grid divided by grid mass.

In **averaged SAR** values, a cube with a defined mass, e.g., 1g or 10g, is used for each point, and power loss density is integrated into this cube. At the end, power loss in integral form is divided by the cube's mass.

SAR computation has been performed with 50 mW input power, and the antenna placed 5 mm above the arm skin. The simulated SARs of the wearable antenna on the arm of the human body at 2.45 and 5.2 GHz are depicted in Fig. 20 (a) and (b). The observed SAR at 2.45 GHz is 0.0691 W/Kg, and at 5.2 GHz is 0.134 W/Kg for 10g tissue, which is far less than IEEE C95.1-2005 standard of 2 W/kg.

This work has been compared with recently reported antennas in Table 2 regarding size, operating frequency, AR, and SAR. According to Table 3 data, this antenna is very compact and provides dual polarization properties. In the future, the antenna, which has dual-band and dual polarization characteristics, is more suitable for communication between the on-body biosensor antennas and the off-body LAN antennas. In ON, the body antenna can collect vital data from biosensor nodes, and in the off-body mode, this antenna communicates with the WiMAX/WLAN antenna to send the data collected from the body sensors to the LAN so that the doctors can take care of their patients remotely. This approach can improve the patient's monitoring quickly and remotely. Remote monitoring will reduce infection spreading and improve patient's mobility and comfort levels.

5. Conclusion

A novel compact dual-band dual-polarized CPW-fed ground circular slot antenna has been designed. Dual-band and circular polarization have been analyzed by introducing inverted T-shaped strips with modified angular ring patch. The measured impedances were 11.22 % and 9.6 % for the lower and upper bands, respectively. The designed antenna provides linear polarization in the lower band while the upper band has circular polarization ability with less than 3 dB AR from 4.85 to 5.4 GHz. The designed antenna is also validated and measured in different scenarios for wearable applications. The simulated SAR is 0.0691 and 0.134 W/Kg at 2.45 GHz and 5.2 GHz respectively. The antenna is expected to be helpful in wireless communication and WBAN systems for wearable applications.

Acknowledgment

The authors gratefully acknowledge Govt. Engineering College, Ajmer, for providing the measurement facilities for this work.

References

[1] Zhang, X. Y., Hang W., Te Mo., and Yun Fei Cao "Dual-band dual-mode button antenna for on-body and off-body communications", *IEEE Trans. Biomed. Circuits Syst*., **11**(4), pp. 933-941(2017). doi: 10.1109/TBCAS.2017.2679048

[2] Chen, M., Gonzalez, S., Vasilakos, A., Cao, H. and et al.,"Body area networks: A survey", *Mob. Netw. Appl.*, **16**, pp. 171-193(2011). doi.org/10.1007/s11036-010-0260-8

[3] Kumar, A., Chaturvedi, D., and Raghavan, S.," Design of a self-diplexing antenna using SIW technique with high isolation," *AEU-Int. J. Electron. Commun.*, **94**, pp. 386-391(2018). doi.org/10.1016/j.aeue.2018.07.031

[4] Nandi S., and Mohan A., "An SIW cavity-backed self-diplexing antenna", *IEEE Antennas Wirel. Propag. Lett.*,**16**, pp. 2708– 2711(2017). doi: 10.1109/LAWP.2017.2743017

[5] Mandal, B., and Parui, S. K.," A miniaturized wearable button antenna for Wi-Fi and Wi-Max application using transparent acrylic sheet as substrate," *Microw. Opt. Technol. Lett.*, **57**(1), pp. 45-49(2015). https://doi.org/10.1002/mop.28781

[6] Mandal, B., Chatterjee A., and Parui, S. K., "Acrylic substrate based low profile wearable button antenna with FSS layer for WLAN and Wi-Fi applications." *Microw. Opt. Technol. Lett*. **57**(5), pp. 1033-1038 (2015). https://doi.org/10.1002/mop.29012.

[7] Wu, D.L., Zhang, G., Li, J.F., and et al., "A low-profile antenna with omnidirectional and unidirectional radiation patterns over two operation bands." *IEEE Access***,** **7**, pp. 182691-182700 (2019). doi: 10.1109/ACCESS.2019.2959821

[8] Tak, J., Woo, S., Kwon, J. and et al., "Dual-band dual-mode patch antenna for on-/off-body WBAN communications", *IEEE Antennas Wirel. Propag. Lett*., **15**, pp. 348-351(2015). 10.1109/LAWP.2015.2444881

[9] Hong, Y., Tak, J. and Choi, J., "Dual-band dual-mode patch antenna for on–on–off WBAN applications", *Electronics Lett.,* **50(**25), pp. 1895-1896 (2014). https://doi.org/10.1049/el.2014.2551

[10] Simorangkir, R.B.V.B., Yang Y., Ladislau M., and et al., "Dual-band dual-mode textile antenna on PDMS substrate for body-centric communications", *IEEE Antennas Wirel. Propag. Lett.* **16**, pp. 677-680 (2016). doi: 10.1109/LAWP.2016.259872

[11] Masood, R., Christian P., and Ronan S., "A dual-mode, dual-port pattern diversity antenna for 2.45-GHz WBAN", *IEEE Antennas Wirel. Propag. Lett*., **16**, pp. 1064-1067 (2016). doi: 10.1109/LAWP.2016.262072.

[12] Tong, X., Liu C., Liu X., and et al., "Switchable ON-/OFF-body antenna for 2.45 GHz WBAN applications", *IEEE Trans. Antennas Propag*. **66**(2), pp. 967-971(2017). doi: 10.1109/TAP.2017.2780984

[13] Gao, G.P., Dou, Z.H., Ma, G and et al. "Dual-band circular patch antenna working in TM41 and TM11 mode for on-/off-body communications", *IET Microw. Antenna Propag*.,**17,** pp. 694-700(2023).doi. org/10.1049/mia2.12376.

[14] Gao, G.P., Dou, Z.H., Yu, Z.Q and et al., "Dual-mode patch antenna with capacitive coupling structure for on-/off-body applications", *IEEE Antennas Wirel. Propag. Lett*., **21(**8), pp. 1512-1516 (2022). doi: 10.1109/LAWP.2022.3170555

[15] Gupta, A., Kansal, A. and Chawla, P., "Design of a compact dual-band antenna for on-/off body communication", *IETE J.Res.*, **69(**2), pp.1013-1021 (2023). doi.org/10.1080/03772063.2020.1845826

[16] Gupta, A., Kansal, A. and Chawla, P., "Design of a patch antenna with square ring-shaped-coupled ground for on-/off body communication", *Int. J. Electron*., **106** (12), pp. 1814-1828 (2019). doi.org/10.1080/00207217.2019.1625970

[17] El Atrash, M., Abdalla, M.A. and Elhennawy, H.M., "A wearable dual-band low profile high gain low SAR antenna AMC-backed for WBAN applications", *IEEE Trans. Antennas Propag*., **67**(10), pp. 6378-6388 (2019). doi: 10.1109/TAP.2019.2923058

[18] Musa, U., Shah, S.M., Majid, H.A., and et al., "Design and analysis of a compact dual-band wearable antenna for WBAN applications", *IEEE Access*, **11**, pp. 30996-31009 (2023). doi: 10.1109/ACCESS.2023.3262298

[19] Gao, G.P., Meng, H.J., Geng, W.F. and et al., "A wideband metasurface antenna with dual-band dual-mode for body-centric communications", *IEEE Antennas Wirel. Propag. Lett*., **21(**1),pp. 149-153(2021). doi: 10.1109/LAWP.2021.3121585.

[20] Chaturvedi, D., Kumar, A. and Althuwayb, A.A., "A dual-band dual-polarized SIW cavity-backed antenna-duplexer for off-body communication", *AEJ - Alex. Eng. J*., **64**, pp. 419-426 (2023). doi.org/10.1016/j.aej.2022.09.021

[21] Mulaparti, M.K., Ratnakumari, U.V. and Satyannarayana, M.,"On body and Off-body performance analysis of an ashoka tree shaped wearable textile antenna for biomedical and military applications", *Radio Sci*., **58(**5), pp. e2022RS007626(2023). doi: 10.1029/2022RS007626

[22] Utsav, A. and Badhai, R.K., "A compact On/Off-Body dual band antenna with modified ground for healthcare applications", *IETE J. Res*. **69(**12), pp. 9266-9277. . DOI: 10.1080/03772063.2022.2098193

[23] Yang, H. and Liu, X. , "Wearable dual-band and dual-polarized textile antenna for on-and off-body communications", *IEEE Antennas Wirel. Propag. Lett*., **19(**12), pp. 2324-2328 (2020). doi: 10.1109/LAWP.2020.3032540.

[24] Zhou, L., Fang, S. and Jia, X.,"Dual-band and dual-polarised circular patch textile antenna for on-/off-body WBAN applications", *IET Microw. Antennas Propag.*, **14(**7), pp. 643-648 (2020). doi.org/10.1049/iet-map.2019.1073

[25] Zhou, L., Fang, S. and Jia, X., "A compact dual-band and dual-polarized antenna integrated into textile for WBAN dual-mode applications", *Prog. Electromagn. Res. Lett.*, **91**, pp. 153-161(2020). https://doi.org/10.2528/PIERL20032901

[26] Gao, G.P., Wang, D., Ma, G., and et al., "A dual-band dual-polarized omnidirectional patch antenna for on-body application", *Microw. Opt. Technol. Lett*., **66(**3), pp. e34050 (2024). https://doi.org/10.1002/mop.34050

[27] Dong, Y., Lu, H. and Chen, X., "A novel dual-band circularly polarized wearable antenna", *Micromachines* , **15**(5), pp. 588 (2024). https://doi.org/10.3390/mi15050\

[28] Saraswat, K. and Harish, A.R., "Flexible dual-band dual-polarised CPW-fed monopole antenna with discrete-frequency reconfigurability", *IET Microw. Antennas and Propag*. **13(**12), pp. 2053-2060 (2019). doi: 10.1049/iet-map.2018.5711

[29] See, T.S., Chiam, T.M., Ho, M.C., and et al. , "Experimental study on the dependence of antenna type and polarization on the link reliability in on-body UWB systems," *IEEE Trans. Antennas Propag*., **60**(11), pp. 5373–5380 (2012). doi: 10.1109/TAP.2012.2208611

[30] Sharma M.D., Yadav A., Singhal S., and et al., "Performance investigation of flexible UWB antenna near human body for wearable appliances," *Prog. Electromagn. Res. B*, **97**, pp. 131-147, (2022). doi:10.2528/PIERB22101109.

[31] Hamed, T., and M Maqsood M., "SAR calculation & temperature response of human body exposure to electromagnetic radiations at 28, 40 and 60 GHz mmWave frequencies", *Prog. Electromagn. Res. M* , **73** , pp. 47-59 (2018). doi:10.2528/PIERM18061102

Figure Caption List

Figure 1. Geometrical Layout of the Designed Dual Band Antenna(a) Front View and (b) Side View

Figure 2. Step-by-Step Progress of Design Process(a) Antenna 1 (b) Antenna 2 (c) Antenna 3 and (d) Antenna 4

Figure 3. Reflection Coefficient (S_{11} in dB) of different Antenna Steps

Figure 4. Axial Ratio (AR in dB) of different Antenna Steps

Figure 5. Current Distribution at (a) 2.45 GHz and (b) 5.2 GHz

Figure 6. The Simulated Current Distributions at 5.2 GHz: (**a)** t= 0; (**b)** t=T/4; (**c)** t= T/2; (**d)** t= 3 T/4

Figure 7.(a) S_{11}(in dB) Plot with R_3 Variation (b). AR (in dB) Plot with R_3 Variation

Figure 8.(a) S_{11} (in dB) Plot with L_{arc} Variation (b) AR(in dB) Plot with L_{arc}Variation

Figure 9.(a) Equivalent Circuit Model of the Proposed Antenna

Figure 9.(b). Reflection Coefficient of the Proposed Antenna in CST EM Simulator and Circuit Simulator.

Figure 10. Measurement Set up with the Fabricated Prototype

Figure 11. Simulated and Measured S_{11} (in dB)

Figure 12. Simulated and Measured AR (in dB)

Figure 13. Radiation pattern at 2.45 GHz for (a) phi 0^o (b) phi 90^o

Figure 14. Radiation pattern at 5.2 GHz for (a) phi 0^o (b) phi 90^o

Figure 15. ON-body Analysis Set up in CST

Figure 16. On-body Performance of the Proposed Antenna at different Gaps from the Phantom Arm

Figure 17. Performance Analysis of the Proposed Antenna without and with Cotton Cloth (a) Reflection Coefficient (b) Axial Ratio

Figure 18. Simulated and Measured S_{11} (in dB) in Free Space and on the Human Arm

Figure 19. Simulated and Measured AR (in dB) in Free Space and on the Human Arm

Figure 20. Simulated SAR on Human Arm at (a) 2.45 GHz and (b) 5.2 GHz

Table Caption List

Table 1. Optimized Dimensions of Proposed Antenna (mm)

Table 2. Dielectric Properties of the Human Body Phantom

Table 3. Comparison between Previously Reported Designs and Current Work

FIGURES

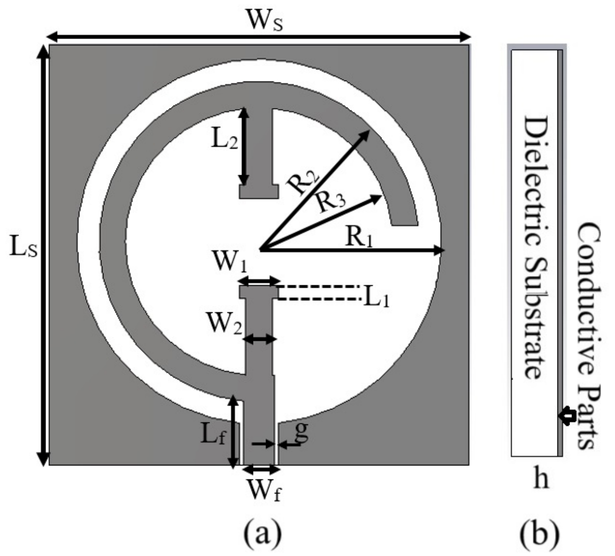

Figure 1. Geometrical Layout of the Designed Dual Band Antenna (a) Front View and (b) Side View

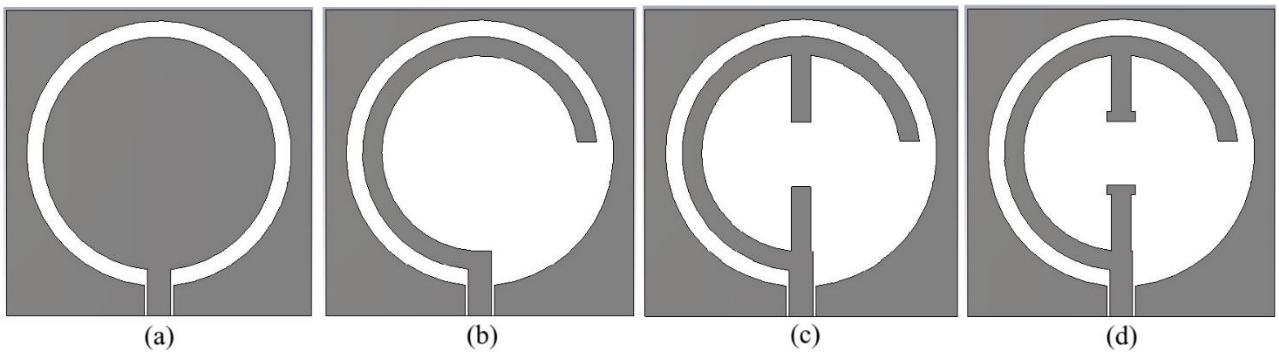

Figure 2. Step-by-Step Progress of Design Process (a) Antenna 1 (b) Antenna 2 (c) Antenna 3 and (d) Antenna 4

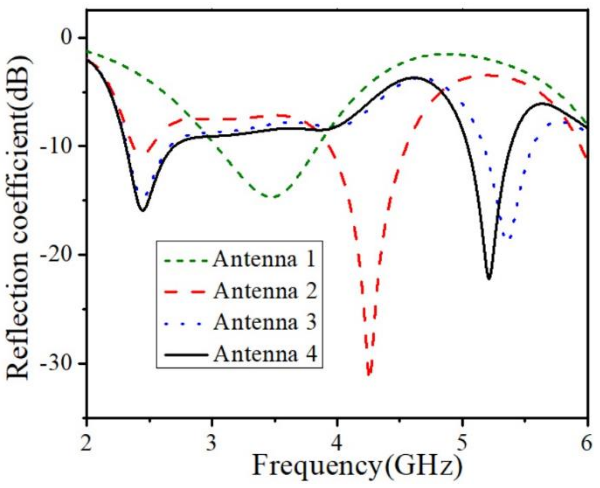

Figure 3. Reflection Coefficient (S_{11} in dB) of different Antenna Steps

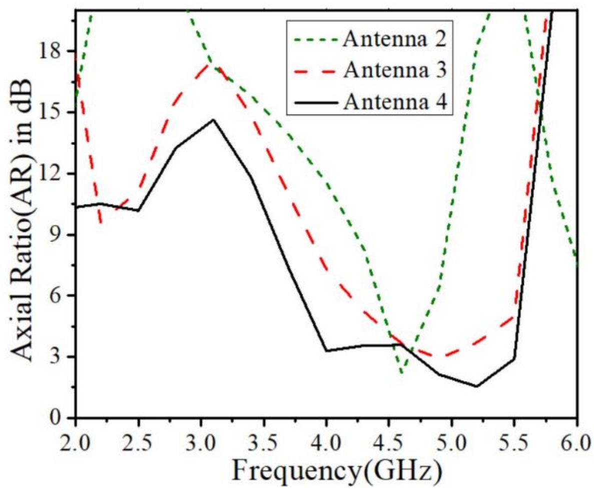

Figure 4. Axial Ratio (AR in dB) of different Antenna Steps

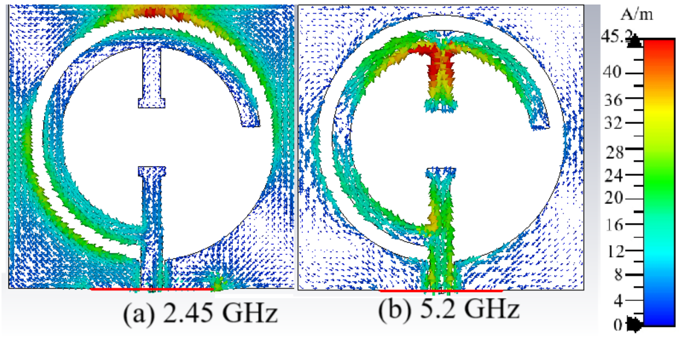

Figure 5. Current Distribution at (a) 2.45 GHz and (b) 5.2 GHz

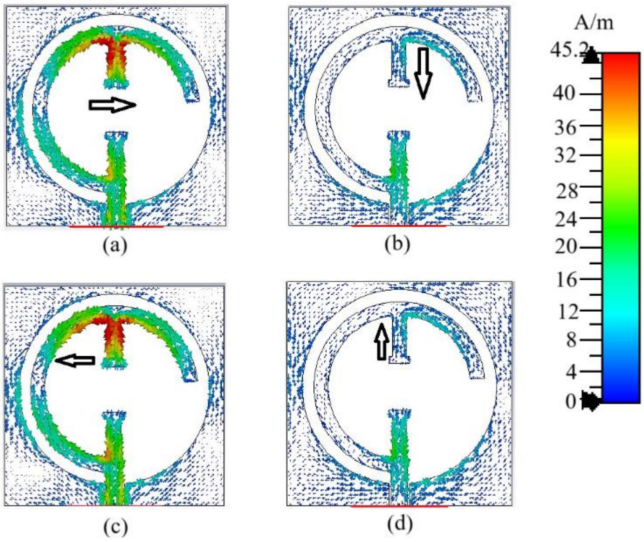

Figure 6. The Simulated Current Distributions at 5.2 GHz: (**a**) t= 0; (**b**) t=T/4; (**c**) t= T/2; (**d**) t= 3 T/4

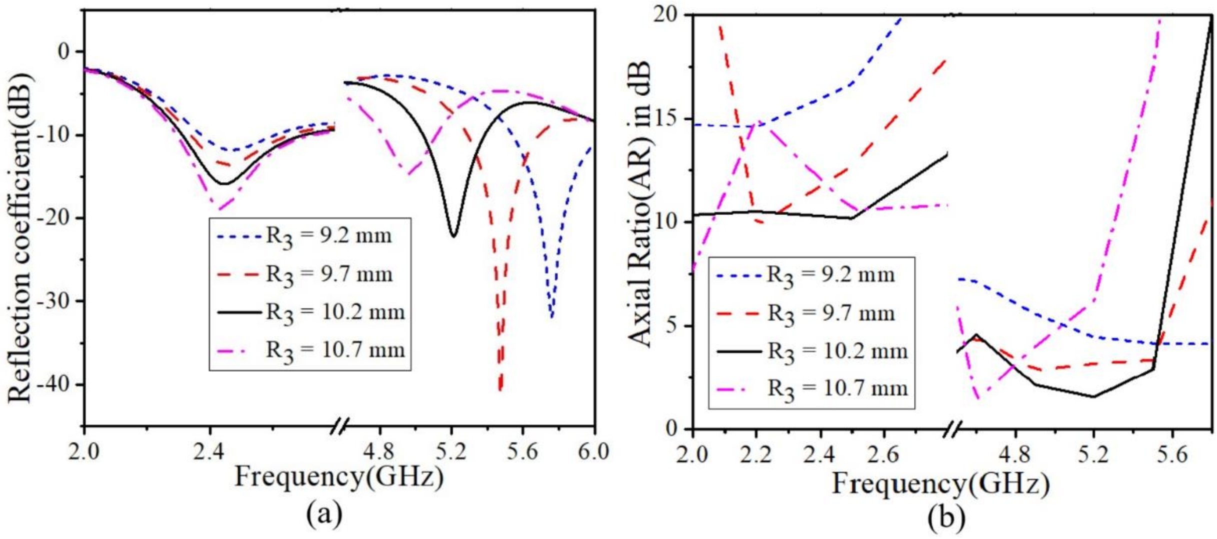

Figure 7(a). S_{11}(in dB) Plot with R_3 Variation **(b).** AR (in dB) Plot with R_3 Variation

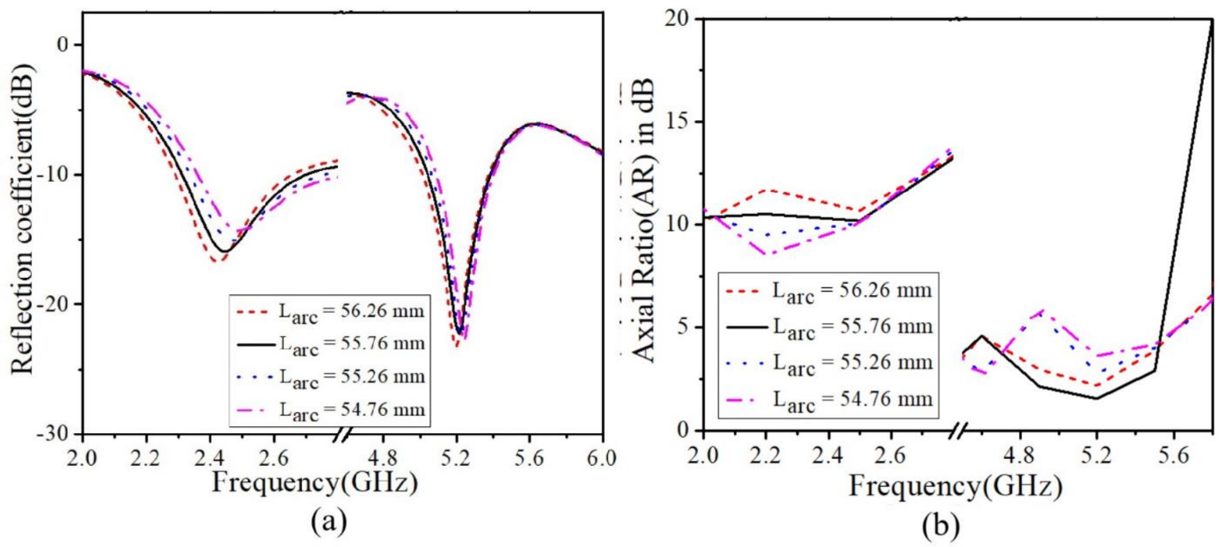

Figure 8.(a) S_{11}(in dB) Plot with L_{arc} Variation **(b)** AR(in dB) Plot with L_{arc}Variation

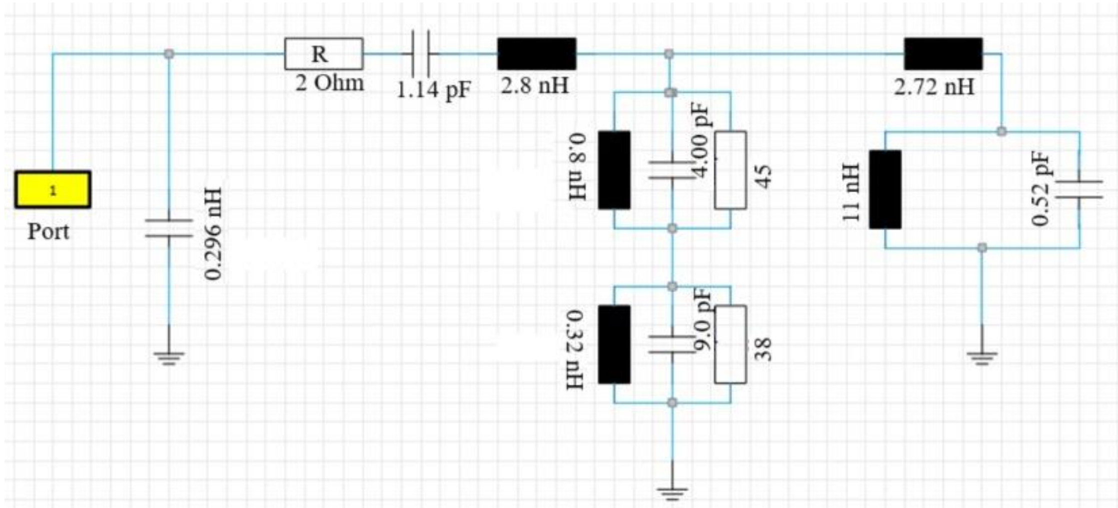

Figure 9(a). Equivalent Circuit Model of the Proposed Antenna

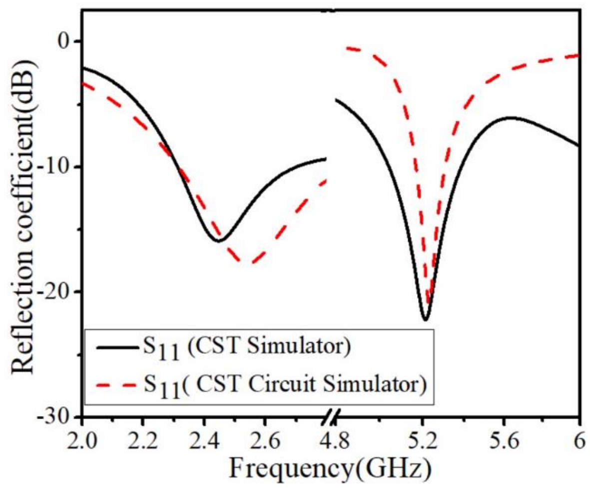

Figure 9(b). Reflection Coefficient of the Proposed Antenna in CST EM Simulator and Circuit Simulator

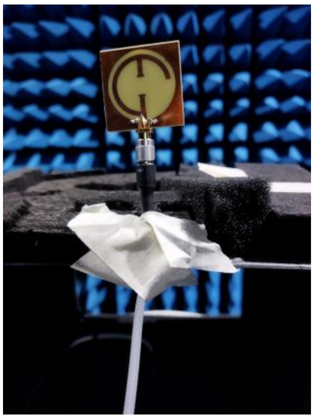

Figure 10. Measurement Set up with the Fabricated Prototype

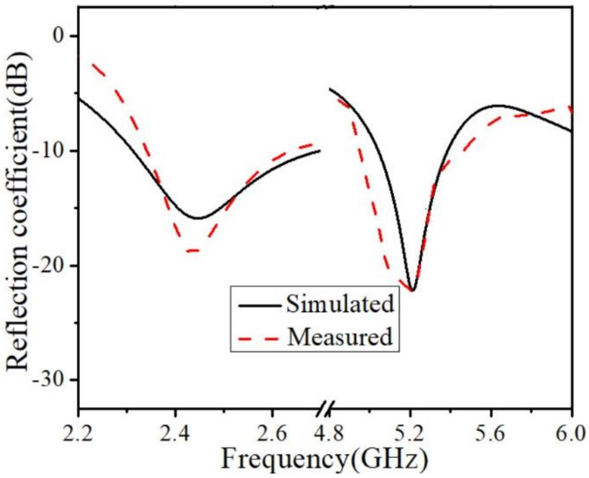

Figure 11. Simulated and Measured S_{11}(in dB)

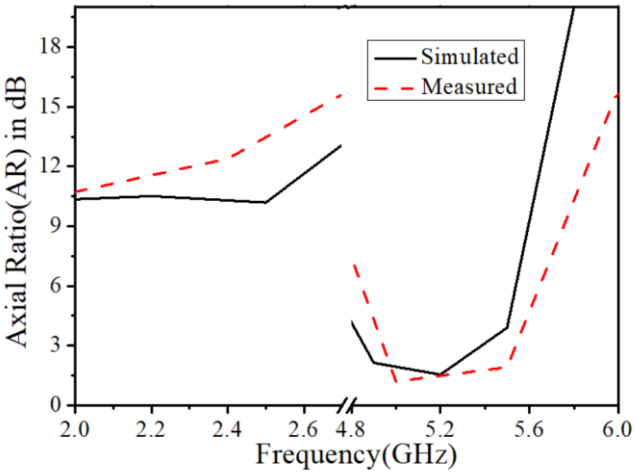

Figure 12. Simulated and Measured AR (in dB)

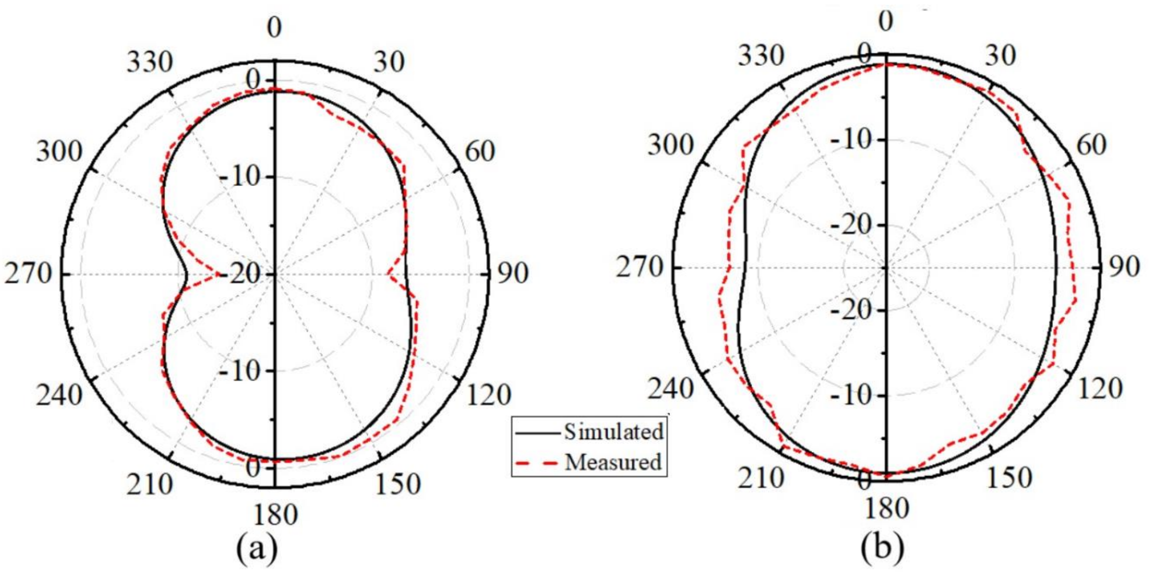

Figure 13. Radiation pattern at 2.45 GHz for (a) phi 0° (b) phi 90°

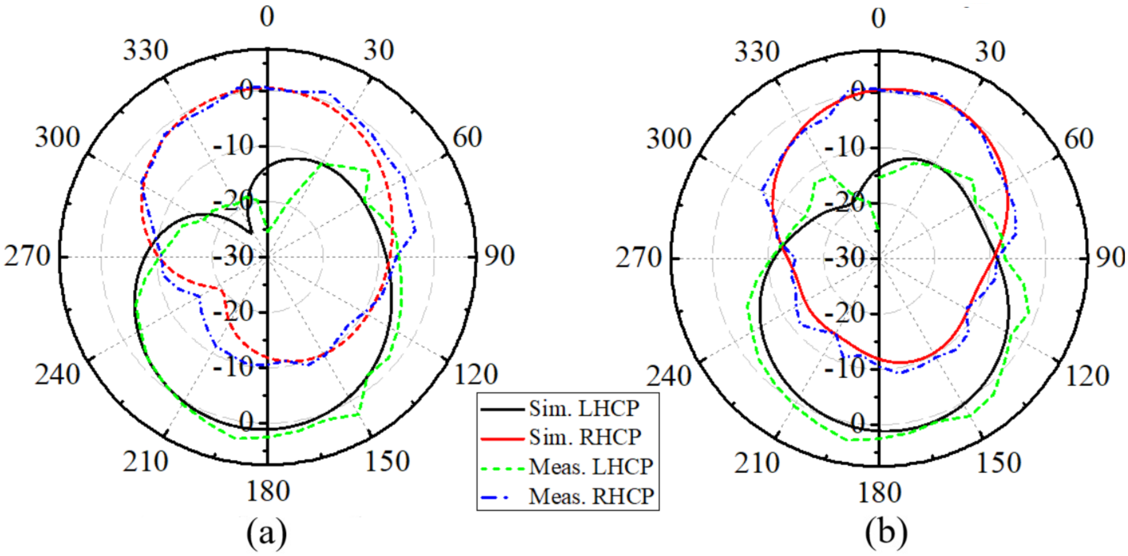

Figure 14. Radiation pattern at 5.2 GHz for (a) phi 0^{o} (b) phi 90^{o}

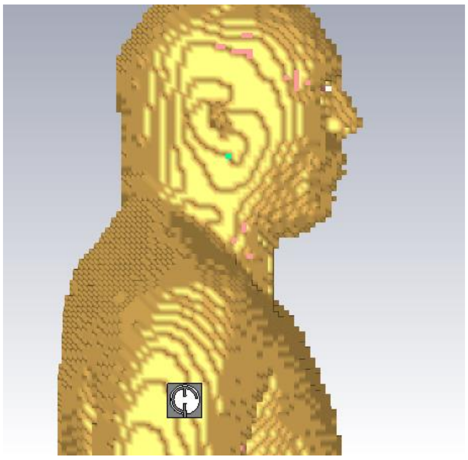

Figure 15. ON-body Analysis Set up in CST

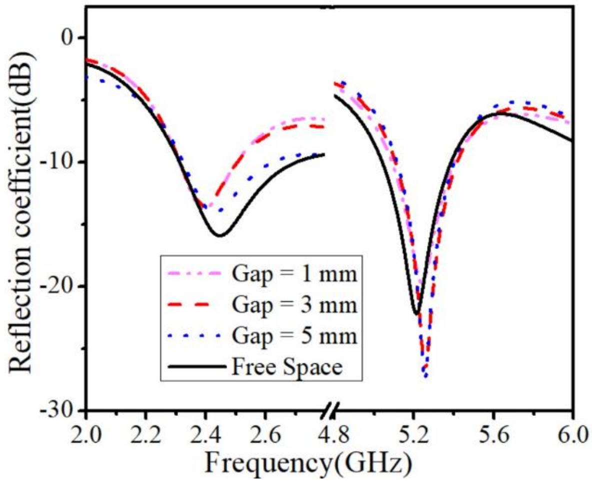

Figure 16. On-body Performance of the Proposed Antenna at different Gaps from the Phantom Arm

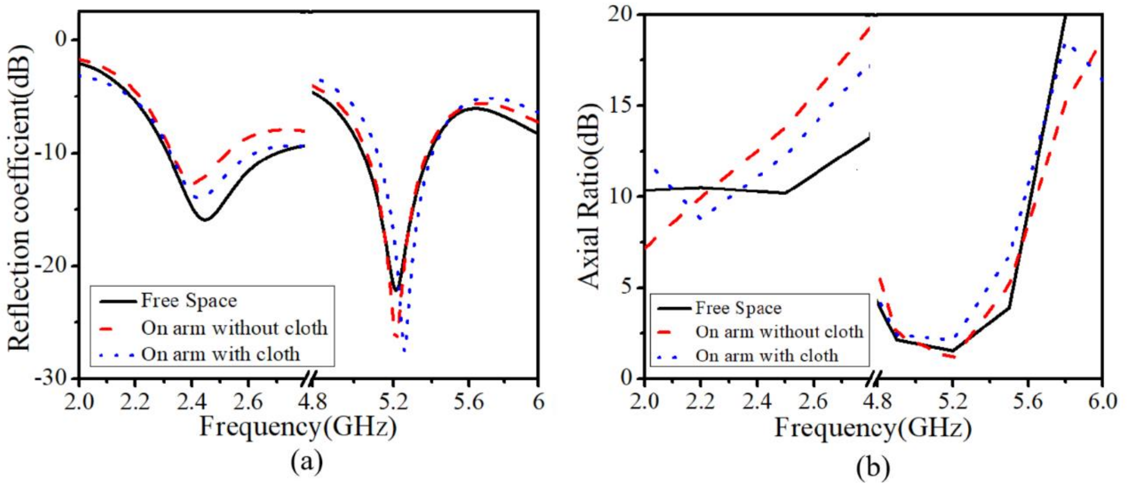

Figure 17. Performance Analysis of the Proposed Antenna without and with Cotton Cloth(a) Reflection Coefficient (b) Axial Ratio

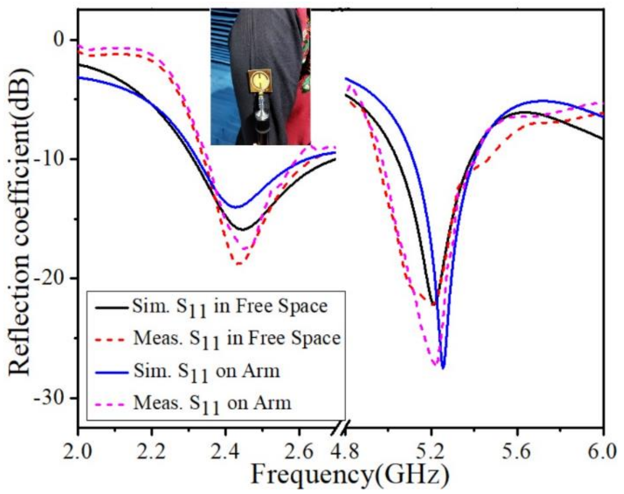

Figure 18. Simulated and Measured S_{11} (in dB) in Free Space and on the Human Arm

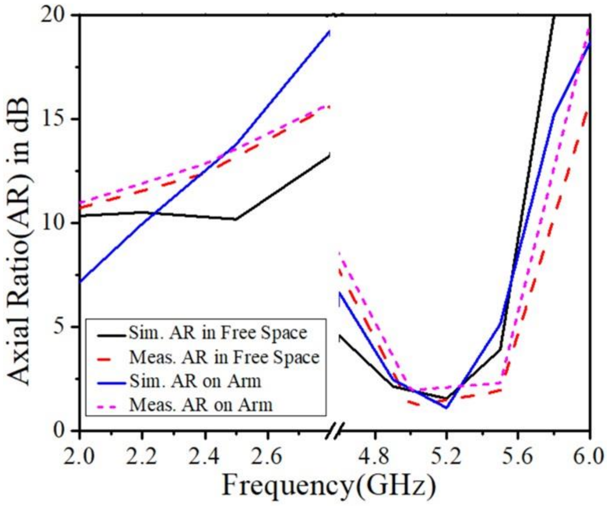

Figure 19. Simulated and Measured AR (in dB) in Free Space and on the Human Arm

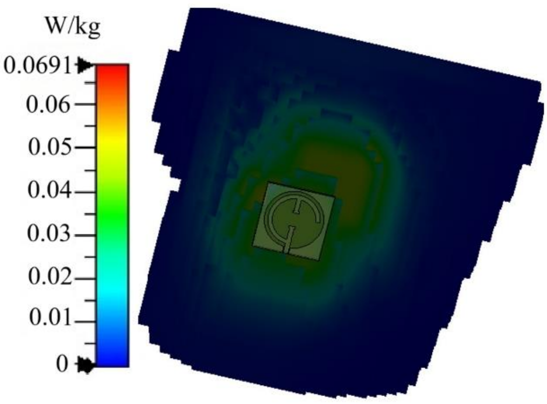

(a) 2.45 GHz and

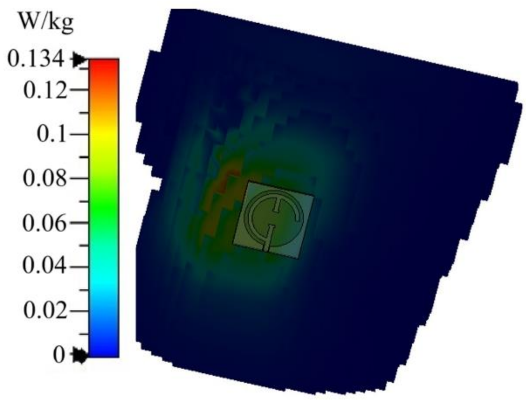

(b) 5.2 GHz

Figure 20. Simulated SAR on Human Arm at (a) 2.45 GHz and (b) 5.2 GHz

Tables

Table 1. Optimized Dimensions of Proposed Antenna (mm)

Parameter	**Size(mm)**	**Parameter**	**Size(mm)**
W_S	32	L_S	32
W_1	3	L_1	1
W_2	2	L_2	5.85
W_f	2.4	R_1	13.9
g_1	0.3	R_2	12.2
h	1.6	R_3	10.2

Table 2. Dielectric Properties of the Human Body Phantom

Tissue Type	**Relative Permittivity**		**Density (kg/m^3)**
	At 2.45 GHz	At 5.2 GHz	
Skin	38	33.4	1100
Fat	5.28	4.91	910
Muscle	52.55	47.6	1041

Table 3. Comparison between Previously Reported Designs and Current Work

Ref [ ]	**Size (mm^3)/ Material**	**Operating Bands (GHz)**	**Polarization**	**Axial Ratio BW (GHz)**	**SAR (W/Kg)**
[15]	15 x28x1.57/ Roger RT 5880	2.3–2.65/ 4.63–5.23	LP/LP	--	1.02/0.524
[16]	38x38x0.6/ FR-4	2.33–2.85 /4.78-5.4	LP/LP	---	0.459/0.303
[18]	41x44x1.52/ Roger Duroid RO3003	2.358-2.447/5.675 - 5.975	LP/LP	---	0.571/0.127
[19]	27.5 x 27.5 x 4/ PDMS	2.40–2.487/ 5.14–5.84	LP/LP	----	0.163/0.0486
[20]	44x44x1.57/ Roger 5880	5.1–5.3/5.68–5.95	LP/CP	5.65-5.95	0.205/0.341
[22]	24 x 22 x1.6/ FR-4	2.34- 2.51/ 4.15-6.35	LP/LP	------	0.118/1.01
[23]	70x70x2/ Felt	2.36–2.40 / 3.4–3.6	LP/CP	At 3.5	0.722/0.53

[24]	100x100x2/ Felt	2.398–2.517 /5.697– 5.915	CP/LP	2.448–2.472	0.042/0.09
[25]	100x100x 4.2 /F4B	2.41-2.473/5.63-6	LP/CP	5.775-5.825	0.254/0.074
IN THIS WORK	32 x32 x1.6/ Fr-4	2.35-2.625/4.95–5.45	LP/CP	4.85-5.4	0.0691/0.134

Biography

Anshul Shrivastava received his B.Tech degree in electronics and communication engineering from NRI Institute of Technology & Management, Gwalior, M.P. India, 2007, and M. Tech degree in Microwave Engineering from Madhav Institute of Science & Technology, Gwalior, M.P. India, 2009. He is pursuing a PhD at the Department of Electronics and Communication Engineering from NERIST Itanagar, A.P. India. His areas of interest are VLSI design, embedded systems, artificial intelligence, machine learning, human-computer interaction, and wearable antennas.

Dr. Ajay Yadav received a B.Tech (AMIETE) degree in Electronics and Telecommunication from IETE, New Delhi, India, in 2008, and an M.Tech degree in Microwave Electronics from the University of Delhi, India, in 2011. He completed a Ph.D. degree in Electronics and Communication from Malaviya National Institute of Technology (MNIT) in 2020, Jaipur, Rajasthan, India. Currently working in the industry in R&D Dept. He has published more than 50 research papers in International/National conferences and peer-reviewed International Journals, He has authored 3 books and 4 book chapters for national and international publishers. He is a Senior Member of IEEE and a Life Member of IETE. He has over 14 Years of experience in Industries (Embedded systems and RF/Microwave) and Academia. He has supervised 6 M. Tech dissertations and is also the “Chhatra Vishwakarma Award 2019” winner as a Mentor. He has also completed a sponsored Project on Bio-degradable RFID Tags. His area of research interest includes the design and analysis of planar antennas, RF/Microwave filters, Conformal Antennas, Phased Array Antenna, UWB Antenna, LNA, Oscillators, power dividers, splitters, Metamaterials, Frequency Selective Surfaces, Reconfigurable antennas, Tera Hertz Communication.

Dr. Rajesh Kumar is presently working as a Professor in the Department of Electronics & Communication Engineering at North Eastern Regional Institute of Science and Technology (Under MHRD, Gov. of India), Nirjuli, Itanagar, India. He received his Bachelor of Engineering in ECE from Bangalore University in 2001, Master of Engineering Science in Control System from NIT, Patna in 2007, and Ph.D. in the field of sensors from Jamia Millia Islamia, New Delhi (A Central University) in 2012.

His area of research is in the field of sensing technology, MEMS, Biosensors, WSN, and Mobile communication. He has 20+ years of teaching experience in various capacities at RPSIT, Patna (Bihar); AKGEC, Ghaziabad (UP) & and ABESEC, Ghaziabad (UP) at undergraduate and postgraduate levels of Engineering Education. He supervised 7 PhD candidates, 12+ MTech Scholars, and 20+ B. Tech projects in his credit. He published more than 75 Research Papers in international/national journals/ conference proceedings.